CHEMISTRY
A EUROPEAN JOURNAL

ChemPubSoc Europe

DOI: 10.1002/chem.201300211

The Photophysics of Pyridine-Derivatized *ortho*-, *meta*-, and *para*-Dibutylamino Cruciforms

Florian Hinderer and Uwe H. F. Bunz*[a]

Abstract: The photophysical properties of a series of *para*-substituted donor–acceptor cruciform fluorophores (***p*1–4**) were investigated and compared with their *meta* and *ortho* isomers (***m*1–4** and ***o*1–4**). The structural variations were found to have a significant effect on the solvatochromism, fluorescence quantum yields (Φ_{fl}), fluorescence lifetimes (τ_{fl}), and response upon addition of trifluoroacetic acid. The observed spectral shifts in absorption and emission caused by protonation of the cruciforms make them promising candidates as chemosensors. Additional computational studies provided more insight into the electronic structure of the systems.

Keywords: cruciforms · distyrylbenzene · fluorophores · solvatochromism · sensors

Introduction

Herein, we describe the effect of positional mutation of the dibutylamino (*ortho, meta,* and *para*) and the pyridyl (2-, 3-, and 4-pyridyl) groups on the optical and electronic properties of a cross-shaped distyrylbenzene fluorophore.

1,4-Distyryl-2,5-bis(arylethynyl)benzenes, (cruciform, XF) are attractive environment-responsive fluorophores.[1] Donor–acceptor substituted XFs, ***p*4** with fully conjugated dibutylamino and pyridine groups, which feature free electron pairs at each terminus, display fascinating double-stage ratiometric color changes upon exposure to metal cations as model analytes.[1] A question, not yet answered, is the influence of the position of the pyridine nitrogen atom and the dibutylamino group on the fluorescence properties of these XFs. If one permutates, nine different positional isomers, namely, ***o*2–4**, ***m*2–4**, and ***p*2–4**, will result. We prepared all of them and investigated their fluorescence properties both in the absence and in the presence of acid. We find surprising trends in this system. By variation of the substitution pattern of the two-dimensional cross-conjugated scaffold, the HOMOs and LUMOs can either be delocalized over the entire molecule or localized to each 1D branch, thus enabling spatial control of electronic properties such as internal charge-transfer (ICT) pathways and the size of the band gap. Such disjoint frontier molecular orbitals (FMOs) make the interaction of cations either with the HOMO or LUMO possible, thus resulting in characteristic changes in absorption and emission. The donor–acceptor substituted XF, ***p*4**, which contains dibutylamino and pyridine groups, displays a two-stage response in fluorescence when exposed to Lewis acids. It is a promising candidate for the design of ratiometric fluorescence sensors. The potential of XFs as luminescent chemosensors led to the synthesis of several types of dyes with spatially separated FMOs, that is, paracyclophanes,[2] distyrylbis(arylethynyl)benzenes,[3] tetrakis(arylethynyl)benzenes,[4] tetraethynylethenes,[5] tetrakis(styryl)arenes,[6] and bis(oxazolo) cruciforms.[7,8] In the case of XFs, the +M and −M-directing substituents were always placed at the *para* position with respect to the connecting styryl and alkynyl groups, respectively.

Bulky *ortho* substituents can distort the planarity of the π-system resulting in a less distinctive electronic conjugation and limited orbital overlap. Although, for *meta*-bridged π-systems, relatively low electronic delocalization is expected in the ground state, rearrangement of the π-orbitals in the excited state can enhance the electronic coupling of the subunits. The photophysical and photochemical behavior of *trans*-stilbenes with either donor or donor–acceptor substituents in the *para* position has been well described in literature, but comprehensive studies for the corresponding *meta* and *ortho* isomers are rare.[9,10] Greater charge-transfer character, longer fluorescence lifetimes, larger fluorescence quantum yields, and smaller isomerization quantum yields were found for *meta*-substituted *cis*- and *trans*-aminostilbenes relative to those found for nonsubstituted and *para*-substituted derivatives.[11] This "*meta*-amino effect" originates from a high torsional barrier for the C−C double bond in the excited state.[12] The same behavior was also observed for other donor-substituted *trans*-stilbenes.[13]

We explored the photophysical behavior of the cruciforms ***p*1–4**, ***m*1–4**, and ***o*1–4** by positional variation of the nitrogen atoms within the aniline and pyridine subunits. We report absorption and fluorescence spectra as well as fluorescence quantum yields and lifetimes of the XFs, ***p*1**, ***m*1**, ***o*1**, and the nine donor–acceptor-substituted XFs, ***p*2–4**, ***m*2–4**, and ***o*2–4**.

[a] Dipl.-Chem. F. Hinderer, Prof. Dr. U. H. F. Bunz
Organisch-Chemisches Institut
Ruprecht-Karls-Universität Heidelberg
Im Neuenheimer Feld 270, 69120 Heidelberg (Germany)
Tel: (+49) 6221-548401
E-mail: uwe.bunz@oci.uni-heidelberg.de

Supporting information for this article is available on the WWW under http://dx.doi.org/10.1002/chem.201300211.

WILEY ONLINE LIBRARY

© 2013 Wiley-VCH Verlag GmbH & Co. KGaA, Weinheim

Results and Discussion

Synthesis: The general synthesis route for both the donor- and donor–acceptor-substituted cruciform, ***p*1–4**, ***m*1–4**, and ***o*1–4**, as reported previously,[1] is outlined in Scheme 1. The precursors for the donor substituents can be afforded in a straightforward two-step synthesis (Scheme 2). While *para*-(dibutylamino)benzaldehyde is commercially available, alkylation of the corresponding bromoanilines, **1** and **2**, followed by a subsequent formylation using *N*,*N*-dimethylformamide (DMF) as the electrophile precursor provides the *ortho*- and *meta*-isomers, **5** and **6**. All alkynylated pyridines are commercially available as their trimethylsilyl-substituted derivatives.

A double Horner olefination of **7** with (dibutylamino)aldehyde **5** and **6** and the *para*-isomer affords 1,4-diiodo-2,5-distyrylbenzenes **8**–**10**, respectively. The ethynyl arms are attached then through a Sonogashira–Hagihara cross-coupling reaction, which employed the 2,3,4-ethynylpyridines and was carried out in THF/diisopropylamine at room temperature with $[Pd(PPh_3)_2Cl_2]$ and CuI as catalysts (see the Supporting Information for details).

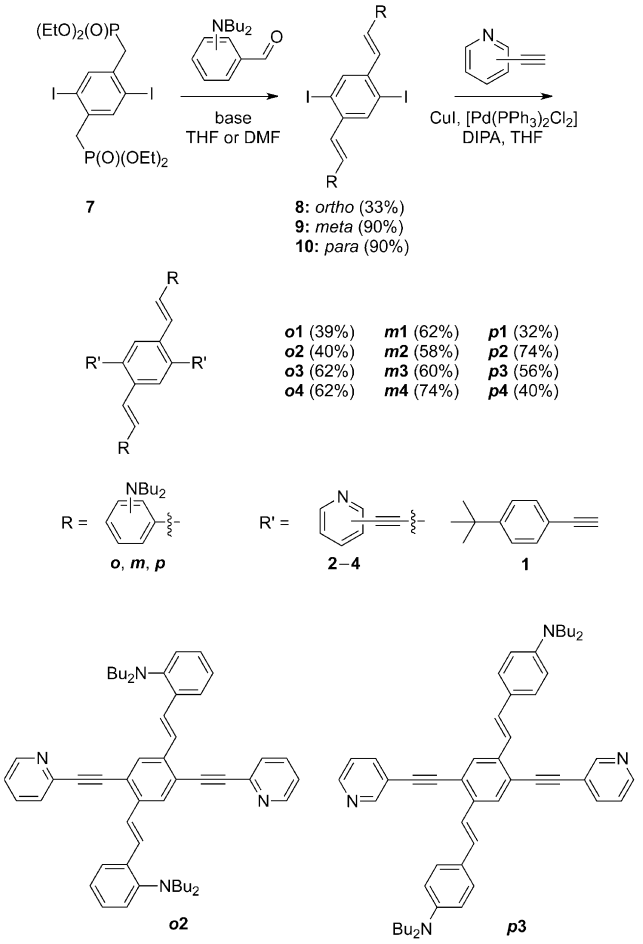

Scheme 1. General synthesis of cruciforms. In the compound labels, the italicized letter (*o*, *m*, and *p*) refers to the position (*ortho*, *meta*, and *para*, respectively) of the dimethylamino group on the styryl axis, whereas the number (**2**–**4**) refers to the position of the pyridine nitrogen atom with respect to the alkyne group. DIPA = diisopropylamine.

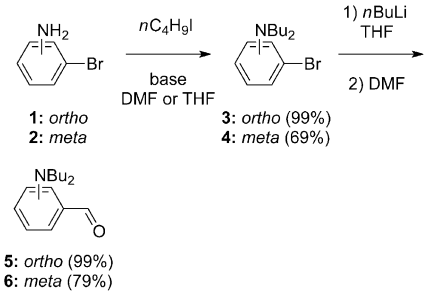

Scheme 2. Synthesis of *ortho*- and *meta*-(dibutylamino)benzaldehydes **5** and **6**.

UV/Vis absorption and fluorescence spectra: Representative for all XFs, the normalized UV/Vis absorption and fluorescence spectra of ***p*4**, ***m*4**, and ***o*4** in *n*-hexane and CH_2Cl_2 are shown in Figure 1. The UV/Vis absorption and fluorescence spectra for all cruciforms are given in the Supporting Information. Whereas the *para* isomer, ***p*4**, displays two broad absorption bands between 300 nm and 550 nm, the *ortho* and *meta* isomers, ***o*4** and ***m*4**, show a single band at approximately 325 nm with low-energy shoulders. The high intensity low-energy band of ***p*4** is attributed to an internal charge-transfer (ICT) transition; the aniline ring in ***o*4** is probably severely twisted out of planarity, owing to steric hindrance, thus leading to a blue-shifted absorption spectrum. Overall, the data show that, in the ground state, everything is as ex-

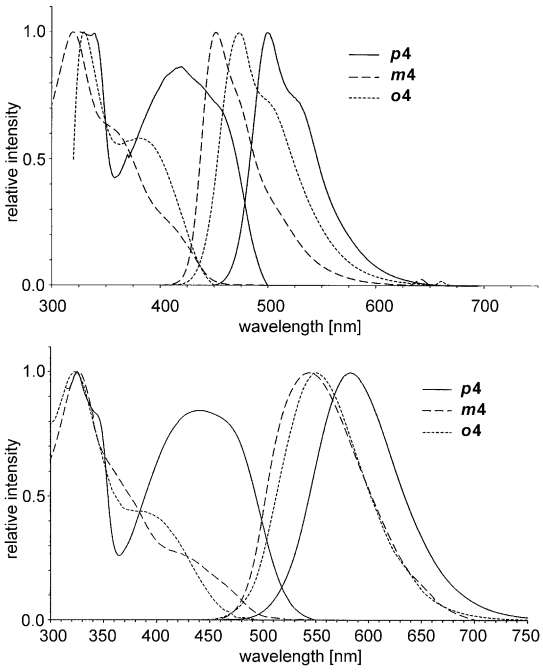

Figure 1. Normalized UV/Vis absorption and fluorescence spectra of ***p*4**, ***m*4**, and ***o*4** in *n*-hexane (top) and CH_2Cl_2 (bottom).

 © 2013 Wiley-VCH Verlag GmbH & Co. KGaA, Weinheim

pected: *meta* substitution suppresses conjugation of the aniline to the styryl nucleus, and the *ortho*-substituted derivatives are twisted, thus pinching off conjugation.

The fluorescence spectra of all isomers display blue emission in nonpolar solvents (e.g. *n*-hexane) with a well-defined vibronic structure for ***p*1–4**, and somewhat structured for ***m*1–4** and ***o*1–4** (see the Supporting Information). All spectra were independent of excitation wavelength. Whereas the emission maxima of the *meta* isomers, ***m*1–4**, in nonpolar solvents are blue shifted (435–451 nm) compared to their *para* isomers, **p1–4**, (465–500 nm) and the *ortho* isomers in polar solvents lie in the range, 461–474 nm, the emission maxima of the *meta* and *ortho* isomers are switched. In contrast to the absorption maxima, the fluorescence maxima reveal a significant positive solvatochromism on going from the nonpolar solvent, *n*-hexane, to the polar solvent, DMF. Large bathochromic shifts for ***p*1–4** (87–109 nm) and ***o*1–4** (93–118 nm), and ***m*1–4** (138–152 nm) are observed, that of the latter being especially remarkable. The data indicate that these species undergo absorption that leads to their conversion from a less polar ground state to a locally excited Franck–Condon state, followed by their relaxation to an energetically low-lying polar ICT state. The small bathochromic shift in absorption (40 nm) for ***p*1–4** with increasing solvent polarity is attributed to an expected polar quinoidal resonance structure in the ground state. The broadened and featureless fluorescence spectra for all isomers in polar solvents also provides evidence for the ICT character of the excited state. The loss of vibrational structure is explained by structural relaxation of the excited state through solute–solvent interactions.

The fluorescence quantum yields (Φ_{fl}) and lifetimes (τ_{fl}) were measured in CH_2Cl_2 and used to estimate the radiative ($k_{fl}=\Phi_{fl}/\tau_{fl}$) and nonradiative rate constants ($k_{nr}=\tau_{fl}^{-1}-k_{fl}$) for all isomers (Table 1). Although moderate fluorescence quantum yields were found for the *para* (0.06–0.40) and *ortho* (0.18–0.28) isomers, ***p*1–4** and ***o*1–4**, the values were substantially lower for the *meta* isomers, ***m*1–4** (0.02–0.12). This observation contradicts the results of Yang and Lewis, who found that *meta*-aminostilbenes had larger fluorescence quantum yields than the corresponding *para* isomers.[10–13] The fluorescence lifetimes were measured by a single-photon counting method and were all well fitted using single-exponential decay curves. According to the results herein, the fluorescence lifetimes of ***m*1–4** (7.6–9.2 ns) are longer than those of ***p*1–4** (1.6–4.4 ns), with those of ***o*1–4** having an intermediate value (3.5–5.1 ns). As a consequence of the low fluorescence quantum yields and long fluorescence lifetimes of ***m*1–4** in comparison to the *para* and *ortho* isomers, only small fluorescence rate constants and large nonradiative rate constants were determined for ***m*1–4** (Table 1), thus resulting in low k_{fl}/k_{nr} ratios. The long fluorescence lifetimes for the *meta* compounds suggest that energy transfers from a donor to an acceptor subunit within one molecule.

Assuming a photoinduced electron transfer (PET) from the donor (aniline) to the acceptor (pyridine) subunit for the *meta* isomers, the long fluorescence lifetimes could be also explained by a slow charge recombination in going from an excited state with an enhanced electronic coupling to an electronically decoupled ground state. As charge recombination is a radiationless process, the low fluorescence quantum yields for ***m*1–4** could also be explained. Another reason for the low quantum yields of the *meta* isomers could also be the existence of one or more conformers, that, with respect to the mono exponential fluorescence decay and the emission spectra being independent of excitation wavelength, are nonfluorescent and only play a negligible role. On the basis of these results, both twisted-intramolecular charge transfer (TICT) and photoisomerization seem implausible.

Table 1. UV/Vis absorption and emission maxima, absorption coefficient (ε), Stokes shift (ν_{Stokes}), fluorescence quantum yield (Φ_{fl}), fluorescence lifetime (τ_{fl}), fluorescence rate (k_{fl}), and nonradiative deactivation (k_{nr}) constants in CH_2Cl_2.

XF	$\lambda_{abs,max}$ [nm]	$\lambda_{fl,max}$ [nm]	ε [$M^{-1}cm^{-1}$]	ν_{Stokes} [cm^{-1}]	Φ_{fl}	τ_{fl} [10^9 s]	k_{fl} [$10^8 s^{-1}$]	k_{nr} [$10^8 s^{-1}$]
***p*1**	340, 440	524	58480	3643	0.40	1.6	2.50	3.75
***p*2**	335, 450	561	46801	4397	0.26	3.9	0.67	1.90
***p*3**	335, 445	548	29492	4224	0.17	3.0	0.57	2.77
***p*4**	338, 441	583	41904	6322	0.06	4.4	0.14	2.14
***m*1**	331	530	91156	11344	0.12	9.2	0.13	0.96
***m*2**	328	552	93544	12372	0.06	8.6	0.07	1.09
***m*3**	325	543	45942	12353	0.05	8.2	0.06	1.16
***m*4**	327	543	60233	12165	0.02	7.6	0.03	1.29
***o*1**	325, 388	523	76672	11649	0.28	3.5	0.80	2.06
***o*2**	324, 388	538	60830	12277	0.21	5.1	0.41	1.55
***o*3**	323, 390	535	60968	12268	0.23	4.8	0.48	1.60
***o*4**	323, 388	550	59756	12778	0.18	4.0	0.45	2.05

Solvatochromism: The absorption and emission spectra of all cruciform, ***p*1–4**, ***m*1–4**, and ***o*1–4** were measured in ten solvents of different polarity, polarizability, hydrogen-bond donor (HBD) and acceptor (HBA) strength. Representatively, Figure 2 shows the absorption and emission spectra of ***o*4** (all spectra can be found in the Supporting Information). The solvent-induced shifts, depending on processes such as nonspecific and specific solute–solvent interactions, were analyzed by a multiple linear-regression analysis (Table 2) according to Kamlet and Taft [Eq. (1)]:[14]

$$\nu_{max} = \nu_o + s\pi^* + a\alpha + b\beta \quad (1)$$

The π^* scale reflects the ability of the solvent to stabilize either a dipole or a charge through nonspecific dielectric interactions. The α and β scales describe specific solute–solvent interactions, α characterizing the hydrogen-bond donor (HBD) strength and β the hydrogen-bond acceptor (HBA) strength of the solvents. Because the absorption maxima for the *meta* and *ortho* cruciforms, ***m*1–4** and ***o*1–4**, are nearly independent of solvent polarity, the Kamlet–Taft analysis was only used to analyze photophysical properties of the emissive state (emission maxima). Here, ν_{max} is the predicted emission maximum in solution, ν_0 is the calculated emission

 © 2013 Wiley-VCH Verlag GmbH & Co. KGaA, Weinheim

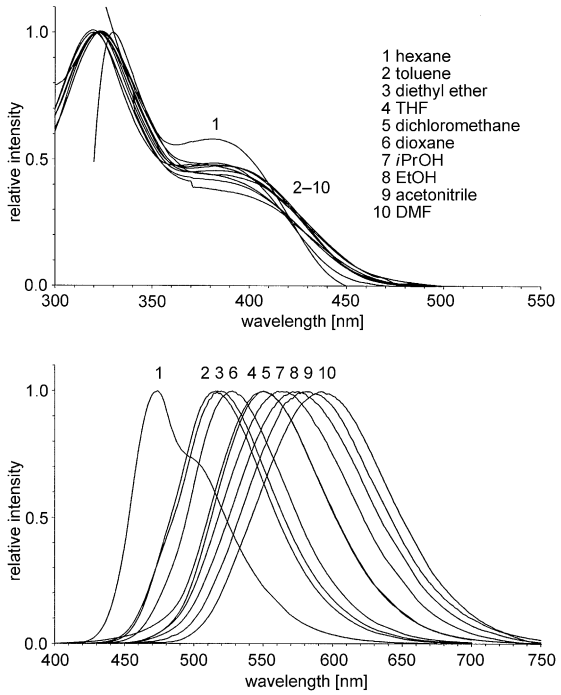

Figure 2. Normalized UV/Vis absorption (top) and emission spectra (bottom) of ***o*4** in a variety of solvents with different polarity.

Table 2. Kamlet–Taft coefficients for the measured emission maxima.

XF	ν_0 [cm^{-1}]	*s*	*a*	*b*	*n*	*r*
***p*1**	21716	−2.890	−1.058	−1.265	10	0.912
***p*2**	20363	−2.964	−0.887	−1.070	10	0.949
***p*3**	20883	−3.127	−0.647	−1.006	10	0.957
***p*4**	21105	−2.831	−1.631	−1.864	10	0.986
***m*1**	23307	−5.080	−1.160	−2.071	10	0.918
***m*2**	21920	−4.674	−0.710	−1.555	10	0.943
***m*3**	22106	−4.762	−0.328	−1.733	10	0.969
***m*4**	21759	−4.000	−0.083	−1.522	10	0.939
***o*1**	21682	−3.062	−0.050	−1.237	10	0.926
***o*2**	21078	−3.252	−0.187	−1.315	10	0.971
***o*3**	21251	−3.288	−0.135	−1.182	10	0.966
***o*4**	21011	−3.456	−0.564	−1.433	10	0.968

maximum in the gas phase and *a*, *s*, and *b* are fitted coefficients (Table 2). The negative values of the coefficients result in a positive solvatochromism for all cruciforms with increasing acidity, basicity, and polarity of the solvents. For the *a* and *b* coefficients, this result is somewhat unexpected. These systems feature four basic groups with free electron lone pairs. However, similar to protonation of the cruciforms through addition of trifluoroacetic acid (TFA), hydrogen bonding between protic solvents and the basic nitrogen atoms of the cruciforms should result in a net blue shift of the emission maxima. But, interruption of that hydrogen bonding because of the amino groups being positively charged (and thus, less basic) in the excited state, leaving only the possibility of hydrogen-bond interactions involving the pyridine groups, could be the reason for the observed bathochromic shift with increasing hydrogen-bond donor strength of the solvents (Table 2). The negative values of the *b* coefficients indicate a higher stabilization of the excited state relative to that of the ground state in basic solvents, resulting in a red shift of the fluorescence maxima. As a resonance structure with a positive charge located on the amino nitrogen atom is expected to be predominant for the excited state, the formation of a Lewis acid–base exciplex involving an excited cruciform and a ground-state Lewis base is plausible.[15] More insight might be obtained by kinetic complexation studies in binary mixtures of hydrocarbons and solvents, which can act as Lewis bases.

The large negative values of the coefficients, *s*, provide evidence for a strong stabilization of the relaxed excited state in polar solvents. The red shift in emission on going from *n*-hexane to DMF correlates well with the excited-state dipole moments of both the cruciforms and the solvents as well as their polarizability. The *s* coefficients of ***o*1–4** are only slightly higher than those of ***p*1–4**, but both of these sets of *s* values are considerably smaller than those of ***m*1–4**. These results indicate larger dipole moment differences between the ground and excited states and therefore larger CT character for the *ortho* and *meta* isomers relative to those for the *para* isomers. One reason for these differences might be the planarization of the more twisted ground-state geometries of ***o*1–4** and ***m*1–4** upon electronic excitation. The extraordinary large difference between the ground and excited-state dipole moments for the *meta* isomers might also arise from a charge separation in the excited state. Instead of being distributed over the whole conjugated π-system, the positive charge would be expected to be located on the nonconjugated amino nitrogen atom and the negative charge on the pyridine subunit.

TFA titration: Cruciform fluorophores, sensitive to protons and metal cations, are potentially attractive as ratiometric chemosensors. The spectral shifts upon addition of TFA by variation of the substituent pattern should give more insight into the photophysical properties of these systems. Figure 3 and Table 3 show the normalized fluorescence spectra of the trifluoroacetic acid (TFA) titrations of the cruciforms in CH_2Cl_2. As expected, the positional variations of the amino and pyridine nitrogen atoms have significant impact on the spectral shifts in absorption and emission upon addition of TFA. At low TFA concentrations, whereas the ICT bands for ***p*1–4** disappear, the absorption spectra of ***m*1–4** and ***o*1–4** only undergo small changes. These results seem reasonable, as protonation of the amino groups lower their donor strength in line with the loss of charge-transfer character. Owing to the lower level of conjugation expected for the *ortho* and *meta* isomers, relative to that expected for the *para* isomer, the absorption and emission characteristics of the latter should exhibit higher sensitivity to the positional variation of the amino and pyridine nitrogen atoms. The increase of TFA content at high TFA concentrations only leads to moderate changes to the absorption spectra of ***p*1–4**, spectra that now resemble those of ***m*1–4** and ***o*1–4**. The

 © 2013 Wiley-VCH Verlag GmbH & Co. KGaA, Weinheim

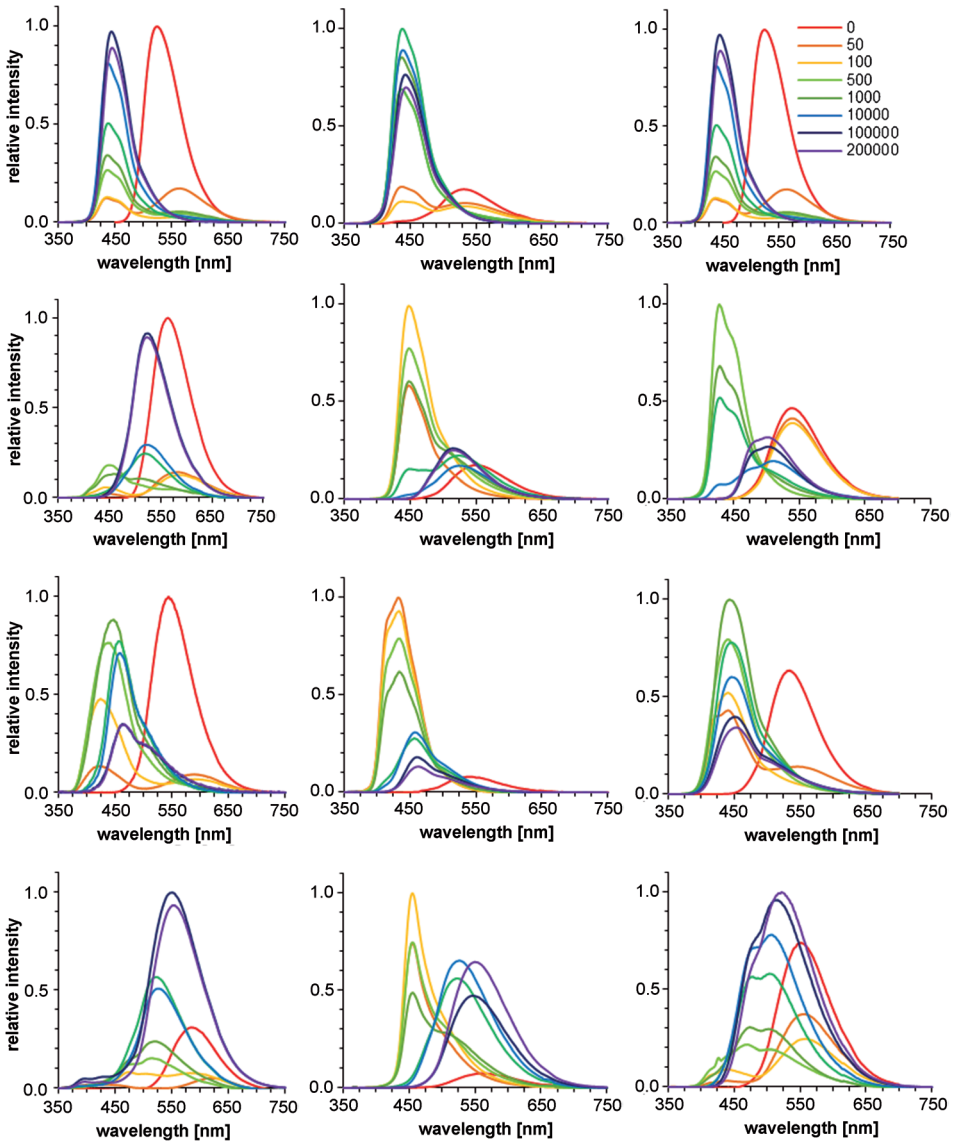

Figure 3. Normalized fluorescence spectra of ***p*1**–***p*4** (top to bottom, left column), ***m*1**–**m4** (top to bottom, middle column) and ***o*1**–***o*4** (top to bottom, right column) in CH_2Cl_2 (1.4 μM) upon addition of different numbers of equivalents of trifluoroacetic acid. Excitation wavelength $\lambda_{exc} = 310$ nm.

position of the pyridine nitrogen atoms has little effect on spectral shifts of the absorption spectra caused by TFA addition. Compared to the absorption spectra, the emission spectra are more sensitive to TFA concentration. According to our previous work, the donor–acceptor substituted cruciforms ***p*2–4**, ***m*2–4**, and ***o*2–4** display a two-stage response in their emission spectra depending on the TFA concentration. All isomers show an initial blue shift caused by protonation of the more basic amino groups, representing a lowering of the energy of the HOMO, followed by a subsequent red shift upon protonation of the pyridine groups, a lowering of the energy of the LUMO. Here, the position of the pyridine nitrogen atom determines the magnitude of the red shift. As expected and attributed to a smaller electronic contribution to the LUMO, the red shifts for ***p*3**, ***m*3**, and ***o*3** are smaller than those of the other isomers. As Figure 4 shows, the changes in fluorescence can be seen by the naked eye. Remarkably, the basicity of the second amino group of the monoprotonated species is obviously not much affected by protonation of the first one. The small difference in the pK_a values of the neutral and monoprotonated XF species is similar to that observed for 4,4′-diamino-*trans*-stilbene, owing to diminished conjugation of the amino groups. Considering both the absorption and the fluorescence spectra, also photoacidity in the excited state is not observed. Interestingly, the *meta* isomers exhibit significant fluorescence turn-on upon addition of small amounts of TFA, a behavior that is even more pronounced in the highly polar solvent, acetonitrile (Figure 4).

As Table 3 shows, the fluorescence intensity ratios, I_1/I_0, upon the addition up to 100 equivalents of TFA in CH_2Cl_2 for ***m*1–4**, lie between 5.7 and 13.4. Additionally, the fluorescence lifetime, τ_{fl}, for the *meta* isomers decreases markedly in the presence of an excess of TFA. This finding is additional evidence for the existence of a PET process. In conjunction with the low fluorescence quantum yields and the long fluorescence lifetimes of the nonprotonated species, these results strengthen the assumption of PET from the donor to the acceptor subunit for ***m*1–4**. But, further experimental investigations will be necessary to prove this hypothesis. What does the study of the *ortho*-, *meta*- and *para*-substituted donor-acceptor cruciforms, ***p*1–4**, ***m*1–4**, and ***o*1–4**, tell us about the effect of N-atom position on the photophysical properties? Whereas only the absorption spectra of the *para*-substituted cruciforms, ***p*1–4**, show a low-energy charge-transfer band, the emission spectra of all XFs reveal internal charge-transfer character. The absorption spectra are quite insensitive to solvent polarity, but in going from nonpolar to polar solvents, the emission bands for all XFs undergo a red shift, broaden, and become featureless. The Kamlet–Taft multiple-regression analysis suggests that the solvent-induced shifts in the emission spectra mostly corre-

 © 2013 Wiley-VCH Verlag GmbH & Co. KGaA, Weinheim

Table 3. Photophysical properties of cruciforms ***p*1**–***p*4**, ***m*1**–***m*4**, and ***o*1**–***o*4** in CH_2Cl_2 upon addition of trifluoroacetic acid. Fluorescence maxima ($\lambda_{fl,max}$), fluorescence lifetime (τ_{fl}), and the ratio of the fluorescence intensities (I_1/I_0 and I_2/I_0).

			50–1000 equiv TFA		excess TFA		
XF	$\lambda_{fl,max}$ [nm]	τ_{fl} [ns]	$\lambda_{fl,max}$ [nm]	I_1/I_0	$\lambda_{fl,max}$ [nm]	I_2/I_0	τ_{fl} [ns]
***p*1**	524	1.6	466	0.35	443	0.97	3.7
***p*2**	561	3.9	449	0.18	523	0.89	3.6
***p*3**	548	3.0	447	0.88	466	0.70	2.4
***p*4**	583	4.4	519	0.24	551	0.93	2.8
***m*1**	530	9.2	439	5.68	444	3.97	3.8
***m*2**	552	8.6	449	5.73	518	1.44	6.1
***m*3**	543	8.2	432	12.50	463	1.65	2.8
***m*4**	543	7.6	455	13.40	550	8.67	3.7
***o*1**	523	3.5	455	2.68	457	2.52	3.3
***o*2**	538	5.1	429	2.15	504	0.68	4.9
***o*3**	535	4.8	443	1.57	454	0.54	3.3
***o*4**	550	4.0	474	0.41	522	1.35	4.7

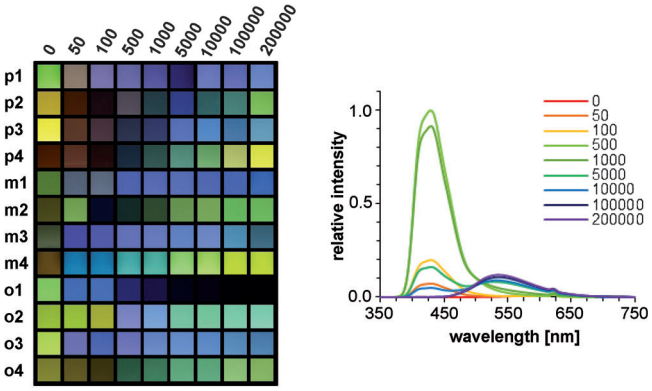

Figure 4. The color of solutions of cruciforms in CH_2Cl_2 after addition of different numbers of equivalents of TFA (horizontal line) under a black light ($\lambda = 366$ nm) and normalized fluorescence spectra of ***m*2** in acetonitrile (2.84 μM) upon addition of different numbers of equivalents of TFA (right).

spond with the ability of the solvent to stabilize a dipole through nonspecific solute–solvent interaction.

The bathochromic shifts for the *meta*-isomers, ***m*1**–**4**, were found to be larger than those for ***p*1**–**4** and ***o*1**–**4**, thus indicating that ***m*1**–**4** have higher charge-transfer character. An explanation for this difference could be charge separation in the excited state, with the positive charge located on the amino nitrogen atom and the negative charge on the pyridine subunit. Unexpectedly, the effect of the hydrogen-bond donor strength on the bathochromic shifts is smaller than that of hydrogen-bond acceptor strength. This result might be explained by a Lewis acid–base exciplex involving the cruciform in the excited state and the ground-state Lewis base. The lower fluorescence quantum yields and longer fluorescence lifetimes for the *meta*-isomers, **m1**–**4**, also suggest the operation of photoinduced electron transfer from the amino donor to the pyridine acceptor subunit. The remarkable fluorescence turn-on and the decreased fluorescence lifetime upon addition of trifluoroacetic acid support this assumption. Whereas the fluorescence intensity ratio, I_1/I_0, and the blue shift of the rising band upon addition of small amounts of TFA can be fine-tuned by the positional variation of the amino nitrogen atom, the position of the pyridine nitrogen atom defines the ratio, I_2/I_0, and the red shift upon addition of larger amounts of TFA.

The puzzle of the red-shifted emission colors of the *meta*-substituted dialkylamino-XFs, **m1**–**4**, is solved by quantum chemical calculations on ***m*1** (B3LYP 6-31G**, Figure 5). The FMOs are not degenerate; HOMO−1 and HOMO as well as LUMO and LUMO+1 are energetically separated. The *meta*-positioned aniline nitrogen atom contributes significantly to the HOMO, that is, the *meta*-dialkylamino substituents are electronically connected to the frame of the XF. The HOMO−1 features dialkylamino substituted benzenes separated from the rest of the conjugated system. LUMO and LUMO+x ($x = 1$, 2, and 3) display the expected distribution, that is, the orbital coefficients are negligible at the *meta* positions in the donor-substituted ring. Our crude calculations, which show surprising delocalization of the HOMO into the *meta*-positioned dialkylanilines, give only a glimpse into the exciting properties of the excited states of ***m*1**–***m*4**.

Conclusion

Meta-positioned dialkylamino groups and nitrogen atoms of pyridine units in cruciforms do not lead to CT bands in the absorption spectra. In the excited state, the conjugation barrier that forbids *meta*-positioned substituents to exert their influence, surprisingly, disappears; thus, ***o*2**–**4**, ***m*2**–**4**, and ***p*2**–**4** differ, in some respect, in their emission spectra (the *meta* compounds generally having lower quantum yields and longer lifetimes, but only slightly less red-shifted emission features), but qualitatively they are similar. The puzzle can be solved, at least partially, if one examines the FMOs of ***m*1** as a representative example. Simple analysis predicts

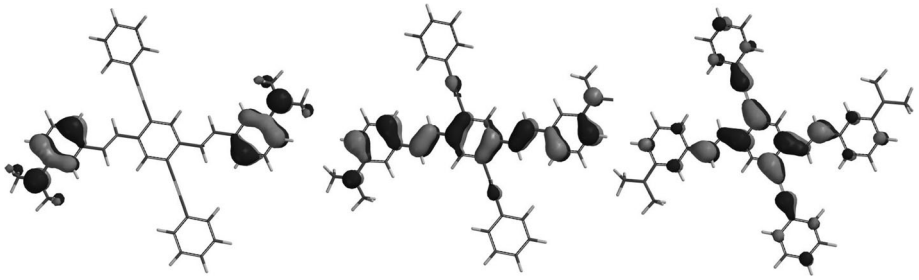

Figure 5. Representation of the HOMO−1 (left), HOMO (middle), and LUMO (right) of ***m*1** (B3LYP 6-31G**, Spartan).

© 2013 Wiley-VCH Verlag GmbH & Co. KGaA, Weinheim

that the energetic positions of HOMO and HOMO−1 reversed, relative to those of the *ortho* and *para*-substituted isomers, as observed in the nonfluorescent bis(3-hydroxystyryl)benzenes.[16] The HOMO encompassing the *meta*-dialkylamino groups conjugates into the XF frame, a situation that is disturbingly different from the example of the *meta*-distyrylbenzenes investigated by Baumgarten, Müllen et al. in their classic paper.[17]

[1] a) A. J. Zucchero, P. L. McGrier, U. H. F. Bunz, *Acc. Chem. Res.* **2010**, *43*, 397–408; b) J. N. Wilson, U. H. F. Bunz, *J. Am. Chem. Soc.* **2005**, *127*, 4124–4125; c) M. Hauck, J. Schönhaber, A. J. Zucchero, K. I. Hardcastle, T. J. J. Müller, U. H. F. Bunz, *J. Org. Chem.* **2007**, *72*, 6714–6725; d) P. L. McGrier, K. M. Solntsev, S. Miao, L. M. Tolbert, O. R. Miranda, V. M. Rotello, U. H. F. Bunz, *Chem. Eur. J.* **2008**, *14*, 4503–4510; e) C. Patze, K. Broedner, F. Rominger, O. Trapp, U. H. F. Bunz, *Chem. Eur. J.* **2011**, *17*, 13720–13725; f) J. Kumpf, U. H. F. Bunz, *Chem. Eur. J.* **2012**, *18*, 8921–8924; g) J. Tolosa, K. M. Solntsev, L. M. Tolbert, U. H. F. Bunz, *J. Org. Chem.* **2010**, *75*, 523–534; h) J. Tolosa, A. J. Zucchero, U. H. F. Bunz, *J. Am. Chem. Soc.* **2008**, *130*, 6498–6506; i) P. L. McGrier, K. M. Solntsev, J. Schönhaber, S. M. Brombosz, L. M. Tolbert, U. H. F. Bunz, *Chem. Commun.* **2007**, 2127–2129; j) J. N. Wilson, M. D. Smith, V. Enkelmann, U. H. F. Bunz, *Chem. Commun.* **2004**, 1700–1701.
[2] G. P. Bartholomew, G. C. Bazan, *Acc. Chem. Res.* **2001**, *34*, 30–39.
[3] J. N. Wilson, M. Josowicz, Y. Wang, U. H. F. Bunz, *Chem. Commun.* **2003**, 2962–2963.
[4] a) E. L. Spitler, L. D. Shirtcliff, M. M. Haley, *J. Org. Chem.* **2007**, *72*, 86–96; b) J. A. Marsden, J. J. Miller, L. D. Shirtcliff, M. M. Haley, *J. Am. Chem. Soc.* **2005**, *127*, 2464–2476.
[5] M. Kivala, F. Diederich, *Acc. Chem. Res.* **2009**, *42*, 235–248.
[6] a) Z. I. Niazimbetova, H. Y. Christian, Y. J. Bhandari, F. L. Beyer, M. E. Galvin, *J. Phys. Chem. B* **2004**, *108*, 8673–8681; b) H. Kang, G. Evmenenko, P. Dutta, K. Clays, K. Song, T. J. Marks, *J. Am. Chem. Soc.* **2006**, *128*, 6194–6205; c) M. Rumi, S. J. K. Pond, T. Meyer-Friedrichsen, Q. Zhang, M. Bishop, Y. Zhang, S. Barlow, S. R. Marder, J. W. Perry, *J. Phys. Chem. C* **2008**, *112*, 8061–8071.
[7] J. E. Klare, G. S. Tulevski, K. Sugo, A. de Picciotto, C. Nuckolls, *J. Am. Chem. Soc.* **2003**, *125*, 6030–6031.
[8] a) J. Lim, O. S. Miljanic, *Chem. Commun.* **2012**, *48*, 10301–10303; b) J. Lim, D. Nam, O. S. Miljanic, *Chem. Sci.* **2012**, *3*, 559–563; c) J. Lim, T. A. Albright, B. R. Martin, O. S. Miljanic, *J. Org. Chem.* **2011**, *76*, 10207–10219; d) K. Osowska, O. S. Miljanic, *Chem. Commun.* **2010**, *46*, 4276–4278.
[9] a) K. M. Gaab, A. L. Thompson, J. Xu, T. J. Martinez, C. J. Bardeen, *J. Am. Chem. Soc.* **2003**, *125*, 9288–9289; b) H. E. Zimmerman, *J. Am. Chem. Soc.* **1995**, *117*, 8988–8991.
[10] J. S. Yang, Y. D. Lin, Y. H. Chang, S. S. Wang, *J. Org. Chem.* **2005**, *70*, 6066–6073.
[11] a) J. S. Yang, K. L. Liau, C. Y. Li, M. Y. Chen, *J. Am. Chem. Soc.* **2007**, *129*, 13183–13192.
[12] a) J. S. Yang, S. Y. Chiou, K. L. Liau, *J. Am. Chem. Soc.* **2002**, *124*, 2518–2527; b) J. S. Yang, K. L. Liau, C. M. Wang, C. Y. Hwang, *J. Am. Chem. Soc.* **2004**, *126*, 12325–12335.
[13] a) F. D. Lewis, J. S. Yang, *J. Am. Chem. Soc.* **1997**, *119*, 3834–3835; b) F. D. Lewis, W. Weigel, *J. Phys. Chem. A* **2000**, *104*, 8146–8153.
[14] a) M. J. Kamlet, J.-L. M. Abboud, M. H. Abraham, R. W. Taft, *J. Org. Chem.* **1983**, *48*, 2877–2887; b) R. W. Taft, W. J. Shuely, R. M. Doherty, M. J. Kamlet, *J. Org. Chem.* **1988**, *53*, 1737–1741.
[15] F. D. Lewis, L.-S. Li, T. L. Kurth, R. S. Kalgutkar, *J. Am. Chem. Soc.* **2000**, *122*, 8573–8574.
[16] K. M. Solntsev, P. L. McGrier, C. J. Fahrni, L. M. Tolbert, U. H. F. Bunz, *Org. Lett.* **2008**, *10*, 2429–2432.
[17] H. Gregorius, M. Baumgarten, R. Reuter, N. Tyutyulkov, K. Müllen, *Angew. Chem.* **1992**, *104*, 1621–1623; *Angew. Chem. Int. Ed. Engl.* **1992**, *31*, 1653–1655.

Received: January 20, 2013
Published online: May 13, 2013

 © 2013 Wiley-VCH Verlag GmbH & Co. KGaA, Weinheim